Heart and Vessels (2019) 34:1230–1239
https://doi.org/10.1007/s00380-018-01338-1

ORIGINAL ARTICLE

The effect of Telmisartan on the expression of connexin43 and neointimal hyperplasia in a rabbit iliac artery restenosis model

Lu Cao[1] · Cui Zhao[2] · Hongliang Cong[1] · Kai Hou[3] · Lianghui Wan[1] · Jixiang Wang[1] · Lili Zhao[1] · Haiyang Yan[4]

Received: 14 November 2018 / Accepted: 28 December 2018 / Published online: 22 January 2019

Abstract

We established a rabbit iliac artery restenosis model to explore the impact of Telmisartan on the expression of Connexin43 (Cx43) and neointimal hyperplasia. Thirty New Zealand white rabbits were randomly divided into three groups: control group ($n=10$), restenosis group ($n=10$), and Telmisartan group ($n=10$). The restenosis model was established by high-cholesterol diet combined with double-balloon injury of iliac arteries. In addition, Telmisartan at 5 mg/(kg day) was administered to the rabbits of Telmisartan group on the second day after the second balloon injury. All rabbits were killed at the end of the experiment followed by institution policy. Before sacrifice, blood samples were obtained to test serum angiotensinII (AngII). Iliac arteries were isolated for morphological analysis and determining the expression of Cx43 by HE staining, immunohistochemical analysis, reverse transcription-polymerase chain reaction (RT-PCR), and Western Blotting analysis. Then, the local AngII levels of arteries were measured by radioimmunoassay. As compared with controls, the expression of Cx43 mRNA (0.98 ± 0.08) vs. (1.27 ± 0.17), $P<0.01$), and Cx43 protein [(0.75 ± 0.08) vs. (0.90 ± 0.08), $P<0.05$] of restenosis group were increased, which were significantly higher than those of Telmisartan group [Cx43 mRNA: (1.27 ± 0.17) vs. (1.00 ± 0.20), $P<0.01$; Cx43 protein: (0.90 ± 0.08) vs. (0.82 ± 0.05), $P<0.05$]. Furthermore, The intima thickness [(266.12 ± 70.27) vs. (2.85 ± 0.19) μm, $P<0.01$] and the local AngII [(115.6 ± 15.7) vs. (90.1 ± 7.7), $P<0.05$] of restenosis group were raised when compared with controls. Telmisartan group exhibited thinner intima compared with restenosis group [(68.22 ± 24.37) vs. (266.12 ± 70.27), $P<0.01$]. However, the local AngII levels between these two groups were approximate. In addition, the plasma concentration of AngII was not significantly different among three groups. In conclusion**,** Telmisartan can inhibit the expression of connexin43 and neointimal hyperplasia in iliac artery restenosis model.

Keywords Restenosis · vascular smooth muscle cells · Neointimal hyperplasia · Angiotensin II · Connexin43 · Telmisartan

Introduction

Percutaneous coronary intervention (PCI) is a main and effective method for coronary artery disease (CAD). However, restenosis is still the Achilles' heel of coronary intervention treatment, which requires further advances understanding of its mechanism and new innovative solutions [1–4]. Restenosis is mainly due to neointima formation [5–7], which is caused primarily by the migration and growth of vascular smooth muscle cells (VSMCs) [8–10]. The gap junction (GJ) consisted of connexins (Cxs) between cells, allowing the rapid exchange of ions, small metabolites, and second messengers, plays crucial roles in the VSMCs disintegration and proliferation [11–13]. Cxs include more than 10 Cxs, which is a conservative family. The major expression of Cxs family in the blood vessel wall is Cx37, Cx40, Cx43, and Cx45. Vascular endothelial cells

Lu Cao and Cui Zhao have contributed equally to this work.

✉ Lu Cao
caolutj@126.com

[1] Cardiology Department, Tianjin Chest Hospital, Tianjin 300222, People's Republic of China

[2] National Center for Cardiovascular Diseases, Fuwai Hospital, Chinese Academy of Medical Sciences and Peking Union Medical College, Beijing 100037, People's Republic of China

[3] School of Medicine, Nankai University, Tianjin 300071, People's Republic of China

[4] Tianjin Key Laboratory of Cardiovascular Remodeling and Target Organ Injury, Pingjin Hospital Heart Center, Affiliated Hospital of Logistics University of the Chinese People's Armed Police Forces, Tianjin 300162, People's Republic of China

predominantly express Cx37 and Cx40. Smooth muscle cells (SMCs) mainly express Cx43, and with a little expression of Cx37 and Cx45. In addition, only certain types of SMCs express Cx40 [14–16]. Studies revealed that the reduction of Cx43 led to the decrease of VSMCs migration and proliferation, which suggested that Cx43 might be a novel target to prevent restenosis after percutaneous transluminal coronary angiography (PTCA) or stent implantation [17–20]. AngiotensinII (AngII) has been proved to be an effective vasoactive peptide, which has impact on the process of VSMCs proliferation and migration by acting Angiotensin II type 1 receptor (AT1R) [21]. Therefore, we ventured the idea that Telmisartan, a specific AT_1R blocker, might act against restenosis by down-regulation of Cxs expression in VSMCs, thus, inhibiting the migration and proliferation of VSMCs. To verify our speculation, we established a double-balloon injury using rabbit iliac artery restenosis model and observed the effect of Telmisartan on pathology, expression of Cx43, and local levels of AngII in restenotic lesions.

Methods

Experimental animals and groups

Thirty 6–12-month-old male New Zealand rabbits (purchased from the Animal Center of Academy of Military Medical Science) were randomly assigned into three groups: control group ($n = 10$), restenosis model group ($n = 10$), and Telmisartan group ($n = 10$). The control group was fed with normal diet for either week. And the other groups were fed with high-cholesterol diet (0.5% cholesterol + 5% lard + 15% egg yolk powder bran) for 8 weeks. The rabbits of Telmisartan group received Telmisartan at a dose level of 5 mg/kg/day by oral gavage from the fourth to the eighth week. The animal experiment was approved and conducted by the ethics committee of Tianjin Chest Hospital in accordance with the guidelines for the care and use of laboratory animals.

Surgical procedures

Rabbits in restenosis model group and Telmisartan group received ketamine (1–2 mg/kg) and haloperidol (5 mg) for induction of anesthesia. The right common carotid artery was isolated and inserted in a 5F artery sheath catheter, and then performed iliac artery arteriography. An appropriate wire-guided balloon catheter (the ratio of balloon diameter to vessel diameter was 1.5:1) was inserted into the right common iliac artery through the 5F artery sheath. The common iliac artery endothelial was injured by the balloon inflated to 10–12 atm. Following that, the balloon was deflated and removed. After removing the sheath, the right common carotid artery and the skin were sutured. Penicillin was given for local anti-infection. All rabbits received gentamicin sulfate (4×105 U/day) intramuscularly in the first 3 days after the surgery for advanced anti-infection. High-cholesterol diet was continued for the operated rabbits.

The second balloon angioplasty was operated 4 weeks later. A selected wire–guided balloon catheter (the ratio of balloon diameter to vessel diameter was 1.1:1) was inserted into the injured common iliac artery through the left common carotid artery. The balloon was inflated to 8 atm for 10 s at the stenosis lesion (stenosis defined as greater than 50%). After angioplasty, the catheter was removed, and the incision was sutured. The method of anti-infection was the same as the first surgery. After the second operation, another 4 week high-cholesterol diet was continued for the survival rabbits.

Four weeks after the second balloon angioplasty, all the rabbits were sacrificed by the method of air embolism. Blood samples were obtained by puncture of the left-ventricular cavity before the rabbits sacrifice for testing the levels of cholesterol and AngII. The iliac arteries were harvested for histologic evaluation and vascular reactivity studies.

Collection of vessels

After rabbits sacrificed, the iliac arteries were isolated and washed with cold normal saline. Each of the iliac arteries was cut into two pieces: the one was fixed with 10% neutral buffered formalin and the other one was stored in liquid nitrogen.

Biochemical analysis

Before sacrifice, blood samples were obtained by puncture of the left-ventricular cavity. Each blood sample was divided into three parts for testing serum cholesterol (CHO) with an autoanalyzer (Type TBA-120FR Toshiba, provided by Tianjin Chest Hospital), plasma AngII concentration by radioimmunoassay (Beijing Atomic Hi-Tech Co., Ltd, China), as well.

Measurements of angiotensin II in Iliac Artery

Iliac artery 100mg was cut into tiny pieces and soaked in the buffers 1000μl (0.05 mmol pH 7.4 PBS + 1% Bovine Serum Albumin), and then homogenized by tissue homogenizer. The homogenate was centrifuged (for 5 min at 12,000 rpm) at 4 °C. Aspirate the supernatant into fresh tubes and store at − 20 °C for later use of AngII quantification by radioimmunoassay.

Morphology and immunohistochemistry

Three sections were chosen from the iliac artery of each rabbit. We performed hematoxylin–eosin (H&E) staining and assessed iliac artery morphology changes. Iliac arteries were isolated and then post-fixed with 10% neutral buffered formalin. Tissue pieces were rinsed for 2 h with PBS and then dehydrated via a series of increased concentrations of ethanol. After that, these tissues were washed with xylene. Tissues were cut into 5 μm sections. These sections were stained with hematoxylin–eosin and immunohistochemistry separately. For immunohistochemistry, the sections were incubated with Cx43 monoclonal antibody (1:1000, Santa Cruz Biotechnology, Inc., USA) in blocking buffer (2% BSA in PBS), then incubated with secondary antibody (Beijing Zhongshan Bio-Tech Co., Ltd, China) for 20 min, and then visualized using DAB (Fuzhou Maixin Biotechnology Development Co., Ltd, China), and counterstained with hematoxylin. Similarly, α-smooth muscle actin (α-SMA) was detected by immunohistochemistry. Iliac arteries were then measured histomorphometrically using an Olympus microscope (Olympus Co., Japan). Measurements were performed using HMIAS-2000 image program (Wuhan Qianping Video Technology Co., Ltd, China). The evaluated parameters included neointimal thickness (the distance between the internal elastic membrane and the lumen), medial thickness (the distance between the inner elastic membrane and the outer elastic membrane), neointimal area (the inner elastic membrane covers the area minus the lumen area), medial area (the outer elastic membrane wraps around the area minus the inner elastic membrane area), and stenosis rate [the area of neointima/(inner elastic membrane) × 100%], as well.

Western blotting

Lysate were prepared in lysis buffer before protein quantification. Samples (22 μl of total protein for Cx43) were run on 12% SDS polyacrylamide gels and electrophoretically transferred to a polyvinylidene fluoride membrane. The membranes were blocked overnight at 4 °C with 5% nonfat dry milk. Subsequently, the membranes were incubated for 2.5 h with anti-Cx43 monoclonal antibody (Santa Cruz Biotechnology, Inc, USA). After washed three times, the membranes were incubated with the secondary antibody (anti-rabbit:1:1000, Beijing Zhongshan Bio-Tech Co., Ltd, China) conjugated to the corresponding horseradish peroxidase-conjugated for 2 h. A chemiluminescence substrate was applied to the membranes which had been washed as just described. Then, the membranes were exposed to X-ray film. Densitometric signals from Western blots were analyzed by NIH image software.

RT-PCR

Total RNA was extracted from vascular tissue with Trizol (Shanghai Shenggong Bio-engineering Co., Ltd, China). The ultraviolet absorbance at 260 nm was measured to determine the amount of RNA. First-strand cDNA was synthesized in a 21 μl reaction system containing 5 μl of total RNA, 1.0 μl of reverse transcriptase (TaKaRa Bio Co. Ltd, Japan), and 2.0 μl oligod T (Shanghai Shenggong Bio-engineering Co., Ltd, China). The reverse transcription was carried out for 60 min at 37 °C followed by a denaturation for 5 min at 95 °C. The products of RT were then stored at – 80 °C. Oligonucleotide primers were shown as below: (1) glyceraldehyde phosphated dehydrogenase (GAPDH): forward: 5-GATGCTGGTGCC GAGTAC-3; reverse: 5-TCGTGGATGACCTTGGCC-3; (2) Cx43: forward: 5-CATTATCTTCATGCTGGTGGTGT-3; reverse: 5-TAATTAGCCCAGTTTTGCTC-3. GAPDH was used as an internal standard. The samples were initially heated to 95 °C for 5 min, and then amplified after 30 cycles as follows: 30 s at 94 °C, 30 s at 57 °C, and then 1 min at 72 °C. The PCR reaction was concluded by 10 min at 72 °C. The PCR products (5–10 μl) were visualized in 2% agarose gel. A solid-state black-and-white video camera was used to capture image, and the Kodak Digital Science ID 2.0 image software was used to analyze the intensity of the bands.

Statistical analysis

SPSS software was used for statistical analyzes. Data are expressed as the mean ± standard deviation for continuous variables. One-way analysis of variance was used to compare difference among groups. $P < 0.05$ was considered to indicate a statistically significant difference.

Results

Changes in body weight

The body weights are shown in Table 1. There were 30 animals in the experiment. During the experiment, one animal in the control group died of diarrhea. Three animals died in the stenosis model group, one of the animals died during the operation, one animal died of diarrhea, and

Table 1 Body weight before and after operation and treatment

Group	*n*	Baseline (kg)	Before sacrifice (kg)
Control	9	2.66 ± 0.16	3.67 ± 0.16
Restenosis model	7	2.70 ± 0.12	3.84 ± 0.18
Telmisartan	7	2.66 ± 0.12	3.82 ± 0.17

Results are expressed as mean ± SD

the other one died of sudden death. Three animals died in the Telmisartan group, one died of diarrhea after surgery, the other two died of sudden death, and the etiology was unknown. Thus, there were, respectively, 9, 7, and 7 animals in the control, restenosis, and Telmisartan groups who entered the result analysis. There was no significant difference in body weight among three groups at baseline ($P > 0.05$). Body weight of all groups increased after 8 weeks, whereas no significant difference among them.

Changes in cholesterol level

The cholesterol concentrations are listed in Table 2. As compared with the controls, restenosis model group, and Telmisartan group exhibited higher serum concentration of CHO ($P < 0.01$). However, the difference of serum lipid concentration was not significant between restenosis model group and Telmisartan group ($P > 0.05$). Our study showed that Telmisartan has no effect on blood lipid levels.

Table 2 Cholesterol and triglyceride level before sacrificed

Group	*n*	CHO (mmol/l)
Control	9	0.58 ± 0.19
Restenosis model	7	20.44 ± 0.68**
Telmisartan	7	20.39 ± 0.60**

Results are expressed as mean ± SD

** $P < 0.01$ vs. control group

Gross pathology

The vessels of control rabbits were pink, thin, and soft. However, the vascular wall of restenosis lesions was hard, white, and thick, which was accompanied with narrow lumen. In Telmisartan group, the vessels show softer vascular wall and larger lumen when compared to those of restenosis model group (Fig. 1).

Histopathologic analysis

As for control group, H&E staining indicated that the intima of iliac artery was consisted of endothelial cells and intimal elastic lamina. Furthermore, VSMCs in the medium arranged regularly. However, H&E staining in restenosis model group showed neointimal hyperplasia with VSMCs' proliferation and internal elastic lamina fracture. In addition, proliferated VSMCs arranged disorderly in the medium and migrated to intima. In Telmisartan group, H&E staining indicated thickened vascular

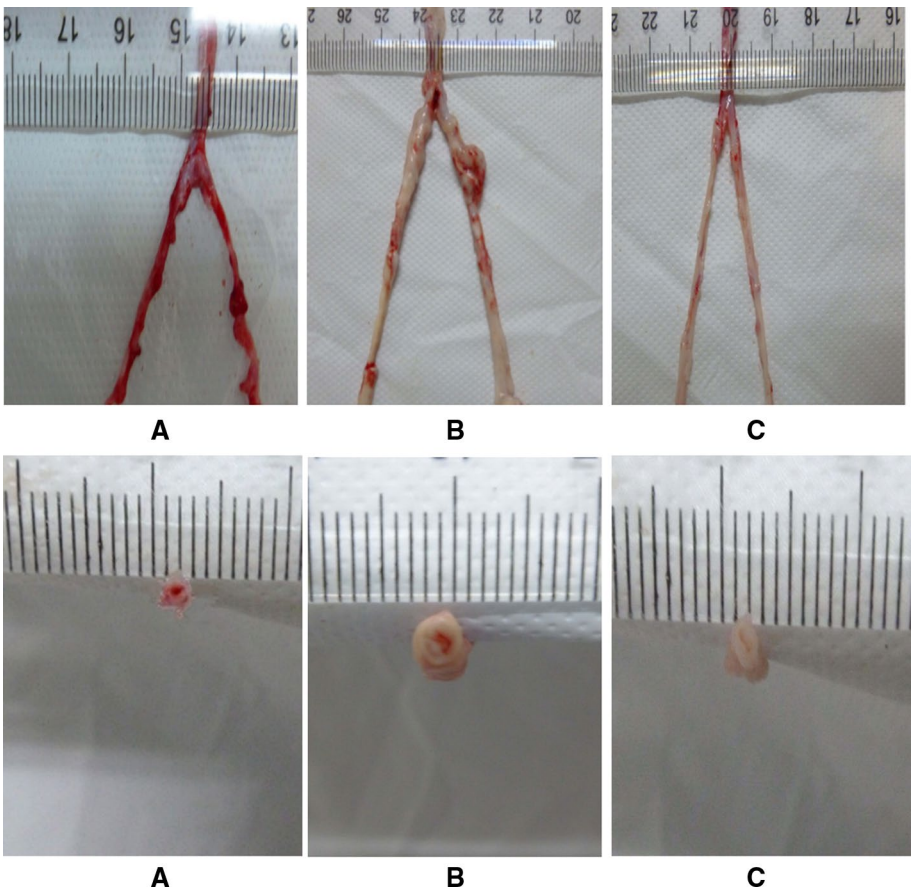

Fig. 1 Gross pathology in control group (**a**), restenosis model group (**b**) and Telmisartan group (**c**)

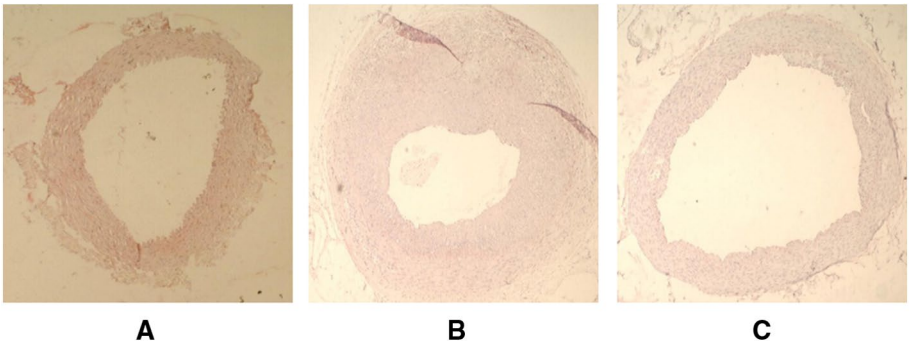

Fig. 2 Hematoxylin–eosin staining of the iliac arteries in the control group (**a**), restenosis model group (**b**) and Telmisartan group (**c**) (magnification × 40)

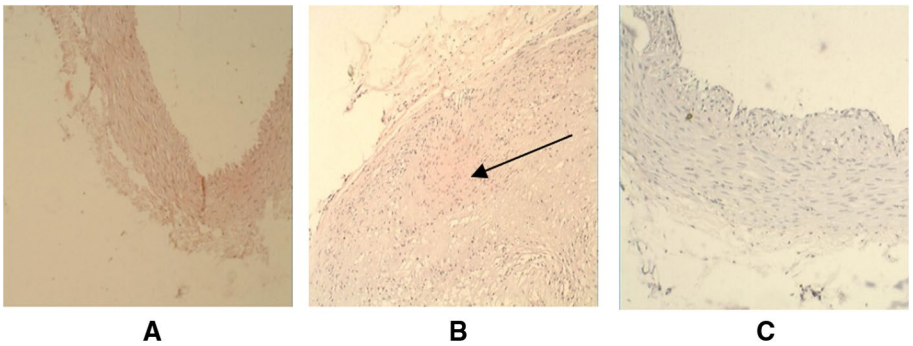

Fig. 3 Hematoxylin–eosin staining of the iliac arteries of control group (**a**), restenosis model group (**b**) and Telmisartan group (**c**) (magnification × 100)

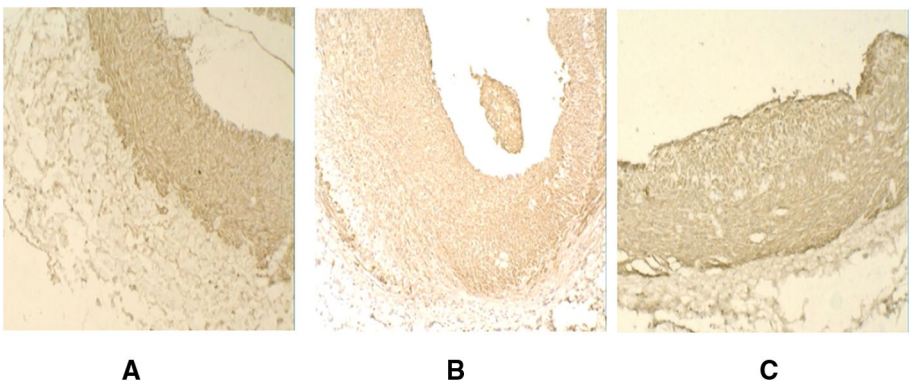

Fig. 4 Immunohistochemical staining of α-SMA in control group (**a**), restenosis model group (**b**) and Telmisartan group (**c**) (magnification × 100)

wall with intact internal elastic lamina. Together with the results of immunohistochemistry, we confirmed that the proliferated cells in neointima are VSMCs in restenosis model group and Telmisartan group (Figs. 2, 3, 4).

Computer-assisted histomorphometric analysis showed the intima thickness of both restenosis model group and Telmisartan group increased compared with that of control group ($P < 0.01$). In addition, as compared with restenosis

Table 3 Neointimal thickness and intima-media thickness ratio

Group	*n*	Neointima (μm)	Intima-media thickness ratio
Control	9	2.85 ± 0.19	0.04 ± 0.17
Restenosis model	7	266.12 ± 70.27**	4.80 ± 1.29**
Telmisartan	7	68.22 ± 24.37**$^{\Delta\Delta}$	1.13 ± 0.34**$^{\Delta\Delta}$

Results are expressed as mean ± SD

** $P < 0.01$ vs. control group; $^{\Delta\Delta}$ $P < 0.01$ vs. restenosis model group

Table 4 Intima-media area ratio and ratio of restenosis

Group	*n*	Intima-media area ratio	Ratio of restenosis
Control	9	0.01 ± 0.00	23.01 ± 3.53%
Restenosis model	7	2.84 ± 0.97**	89.32 ± 6.93%**
Telmisartan	7	0.71 ± 0.34**$^{\Delta\Delta}$	42.56 ± 18.12%**$^{\Delta\Delta}$

Results are expressed as mean ± SD

** $P < 0.01$ vs. control group ,$^{\Delta\Delta}$ $P < 0.01$ vs. restenosis model group

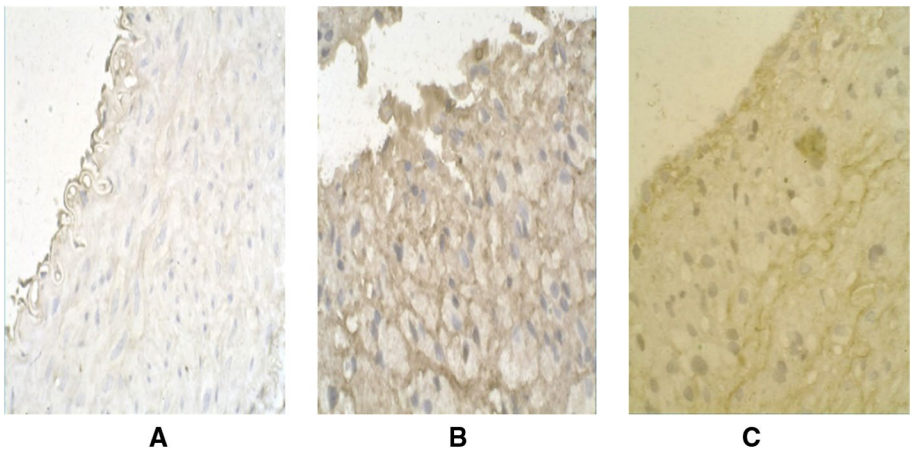

Fig. 5 Immunohistochemistry for connexin43 (Cx43) in the rabbit iliac arteries in different groups (**a** control group, **b** restenosis model group, **c** Telmisartan group) (magnification × 400)

Table 5 AngII level (pg/ml) in plasma and iliac tissues

Group	*N*	Ang II	
		In iliac tissue	In plasma
Control	9	90.1 ± 7.7	394.45 ± 59.45
Restenosis model	7	115.6 ± 15.7*	396.89 ± 101.66
Telmisartan	7	123.8 ± 22.1*	313.51 ± 96.22

Results are expressed as mean ± SD

*$P < 0.05$ vs. control group

model group, Telmisartan group exhibited thinner intima ($P < 0.01$) (Tables 3, 4).

Immunohistochemical analysis indicated that Cx43 was expressed in iliac arteries of three groups. As compared with the controls, higher Cx43 expression was detected in neointima and media in restenosis model group and Telmisartan group. And the quantity of Cx43 expression in Telmisartan group was lower compared with that of restenosis model groups (Fig. 5).

AngII level

The local concentrations of AngII are enhanced in restenosis model group and Telmisartan group when compared with those of controls ($P < 0.05$). However, there is no difference between the two experiment groups. In addition, the plasma concentrations of AngII are not significantly different among three groups (Table 5).

Western blotting

Compared with control group and Telmisartan group, the expression of Cx43 protein increased significantly in restenosis model group ($P < 0.05$) (Table 6 and Fig. 6).

Table 6 Relative optical density of the Cx43 of different groups

Group	*n*	Cx43
Control	9	0.75 ± 0.08
Restenosis model	7	0.90 ± 0.08*
Telmisartan	7	0.82 ± 0.05$^{\triangle}$

Results are expressed as mean ± SD

*$P < 0.05$ vs. control group; $^{\triangle}$ $P < 0.05$ vs. restenosis model group

RT-PCR

Comparing with control group and Telmisartan group, the expression of Cx43 mRNA increased in restenosis model group ($P < 0.01$, respectively). Telmisartan group showed higher Cx43 mRNA expression than that of control group, but the difference was not statistically significant (Table 7 and Fig. 7).

Discussion

Percutaneous coronary intervention (PCI) has gradually become the most common method for revascularization in patients with coronary heart disease [22, 23]. However, the

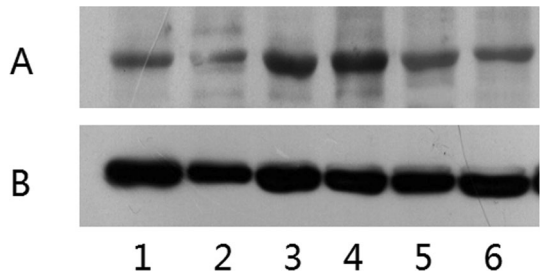

Fig. 6 Protein expression of Cx43 in the rabbit iliac arteries of different groups. Top panels (**a**) represented protein expression of Cx43 of each group and bottom panels (**b**) were β-actin. Control group (1–2), restenosis model group (3–4), Telmisartan group (5–6)

Table 7 Relative optical density of the amplified products of Cx43 in different groups

Group	*n*	Cx43
Control	9	0.98 ± 0.08
Restenosis model	7	1.27 ± 0.17**
Telmisartan	7	1.00 ± 0.20$^{\Delta\Delta}$

Results are expressed as mean ± SD

** $P < 0.01$ vs. control group; $^{\Delta\Delta}$ $P < 0.01$ vs. restenosis model group

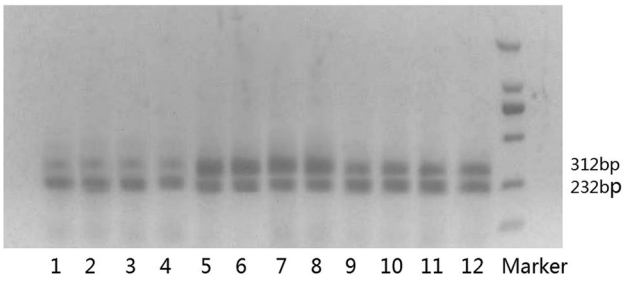

Fig. 7 mRNA expression of Cx43 in the rabbit iliac arteries of different groups. Top panels represented mRNA expression of Cx43 of each group and bottom panels were GAPDH. Normal control (1–4), restenosis model group (5–8), Telmisartan group (9–12)

intervention site restenosis limited its long-term efficacy [24]. Actually, restenosis is a local vascular overreaction during healing after injury and neointimal hyperplasia is considered as the main reason of restenosis. Furthermore, VSMCs may play an important role in the development of neointima formation. VSMCs migrate from the media to the intima and proliferate under the intima, which was considered to be the main cause of restenosis after angioplasty [13, 25].Cells in the injured vascular after angioplasty, especially VSMCs in tunica media, were activated by mechanical injury and mitogenic factors activate and accumulation of growth factor. Then, activated VSMCs switched from the contractile phenotypic state to a non-contractile (synthetic, highly proliferative, and migratory) phenotype [26]. Transformed VSMCs proliferated, migrate to the source of stimulation, and ultimately led to neointima hyperplasia [27–29]. In our study, the vessels of control rabbits were pink, thin, and soft. H&E staining indicated that the intima consists of endothelial cells and intimal elastic lamina and VSMCs in the medium arranged regularly. However, the vascular wall of restenosis lesions was hard, white, and thick, accompanied with narrow lumen. H&E staining also showed neointimal hyperplasia with VSMCs proliferation and internal elastic lamina fracture. In addition, VSMCs in the medium proliferated, arranged disorderly, and migrated to intima. Using the method of immunohistochemistry to detect α-smooth muscle actin (α-SMA), we confirmed that the proliferated cells in neointima are VSMCs. Since these features accorded with pathologic changes in restenosis models, we confirmed that our research established restenosis model successfully through high-cholesterol diet and double-balloon injury in rabbit iliac artery.

SMCs mainly express Cx43 [14–16]. Recently, great interest has been aroused in research on Cx43 and restenosis. The association between Cx43 and neointima formation following balloon angioplasty in rat carotid artery was first investigated by Yeh et al. [30], for whom observed that the changes in activation and phenotype of intimal SMCs paralleled with increased expression of Cx43. Han et al. [18] established carotid balloon injury model, which certified the vital role of Cx43 in the pathogenesis of vascular restenosis, and provided new perspective on the development of vascular restenosis. Through isolated SMCs from the coronary artery of pigs with restenosis and control group, Zhang et al. [31] were demonstrated that Cx43 levels are associated obviously with the SMC phenotypic change and migratory pattern. It is suggested that Cx43 will probably become a new target in restenosis therapy, which is consistent with the results in our research. Immunohistochemical analysis indicated that Cx43 expressed in all iliac arteries of three groups. As compared with controls, higher Cx43 expression was detected in neointima and media in restenosis model group and Telmisartan group. In addition, the Cx43 expression of Telmisartan group was lower than that of restenosis model groups. RT-PCR and western blotting in these groups revealed the same results.

Renin–angiotensin system (RAS) plays a crucial role in the development and progression of restenosis. It was proved that after PCI, the injured blood vessel walls' local RAS was activated, and AngII gene expression and protein synthesis increased, and then, AngII worked with growth factors and multiple cytokines to promote cell migration, proliferation, and hypertrophy of VSMCs [32–34], which is consistent with our study.

From what have discussed above, we can conclude that VSMCs are crucial in the pathogenesis of restenosis after vascular injury. With the process of neointima formation, RAS and the express of Cxs may play important roles. However, it is uncertain whether there is an association between RAS activity and the express of Cxs. By observing Gap junction between human saphenous vein SMCs, Jia et al. [35] found that the expression of Cx43 increased through MAPK-AP-1 signaling pathway, after AngII acting on AT1R. Behind renin-dependent and -independent hypertension model were constructed, respectively, Alonso et al. [36] conclude that AngII increased Cx43 in renin-dependent hypertension selectively by activating extracellular signal-regulated kinase and NF-Kb pathways. Through utilized Sprague–Dawley rats' myocardial infarction model, Hou

et al. [37] suggested that the expression of Cx43 in cardiac stem cells after transplantation post MI regulated through the ANGII/AT1R/TGF-beta1 signaling pathway. Liu et al. [38] were isolated mesenchymal stem cells and endothelial cells from Sprague–Dawley rats, and they found that AngII pretreatment increased the Cx43 expression. Our research showed that the local levels of AngII were enhanced in restenosis model group when compared with those of controls [(90.1 ± 7.8) vs. (115.6 ± 15.7), $P < 0.05$]. In addition, the plasma levels of AngII difference between the two groups were not significant. Moreover, comparing with control group, the expression of Cx43 mRNA [(0.98 ± 0.08) vs. (1.27 ± 0.17), $P < 0.01$] and Cx43 protein level [(0.75 ± 0.08) vs. (0.90 ± 0.08), $P < 0.05$] both increased in restenosis model group. Thus, the possible mechanism of restenosis might be: activated local RAS with elevated AngII level induced by balloon injury upregulated Cx43 expression through AT1R, which lead to enhancement of the exchange of information, materials, and energy among cells. The enhanced cellular communication could stimulate the migration and proliferation of VSMCs, which would promote neointimal hyperplasia, and then restenosis occurred.

Many studies have shown that renin–angiotensin–aldosterone system (RAAS) inhibitors, especially ARBs, would be effectively suppressed restenosis after PCI [39–41]. The VAL-PREST trial [40] reported the prominent treatment effects of Valsartan on restenosis in complex coronary lesions after stenting. In this study, compared with the patients in the placebo group who were taking angiotensin-converting enzyme inhibitor (ACEI), the Valsartan was more effective in preventing in-stent neointimal proliferation. In addition, Valente et al. [41] showed that the proliferation and migration of VSMCs induced by AngII was detected by AT1R/nicotinamide adenine dinucleotide phosphate oxidase 1/interleukin-18 signal pathways, and this effect can be attenuated by losartan. After examining the in-stent neointimal thickness of hypercholesterolemic New Zealand white rabbits, Ichikawa et al. [42] have shown that neointimal formation in the stented carotid arteries of rabbits could be suppressed by systemic administration of ARBs. Cho et al. [43] demonstrated the anti-proliferative and anti-inflammatory effects of ARBs, after evaluating the neointimal features of stent restenosis by optical coherence tomography (OCT), the ARBs group showed fewer number of uncovered stent struts and less amount of neointimal area during follow-up. Different from their studies, Xie et al. [44] conducted a meta-analysis to evaluate benefits of ARBs in patients after coronary stenting. After included 624 patients, the final results showed that ARBs has no significant effect to inhibit neointimal hyperplasia. However, there is rarely study focused on the effect of Telmisartan on restenosis so far. In our study, we established restenosis model successfully through high-cholesterol diet and double-balloon injury in rabbit iliac artery. In Telmisartan group, the vessels show softer vascular wall and larger lumen when compared with the restenosis model group. Furthermore, Telmisartan group revealed lower thinner intima [(68.22 ± 24.37) vs. (266.12 ± 70.27) μm, $P < 0.01$], stenosis rates [(42.56 ± 18.12)% vs.(89.32 ± 6.93)%, $P < 0.01$], expression of Cx43 mRNA [(1.00 ± 0.02) vs. (1.27 ± 0.18), $P < 0.01$], and Cx43 protein [(0.90 ± 0.08) vs. (0.82 ± 0.05), $P < 0.05$] when compared with restenosis group. These results indicated that Telmisartan might inhibit the migration and proliferation of VSMCs by specifically blocking the binding of AT1R to AngII and then down-regulating the express of Cx43 in vascular wall.

Conclusion

This research established restenosis model successfully through high-cholesterol diet and double-balloon injury in rabbit iliac artery. The possible mechanism of our restenosis model might be: activated local RAS induced by balloon injury upregulated Cx43 expression through AT_1R, which led to enhancement of the exchange of information, materials, and energy among cells. The enhanced cellular communication could stimulate the migration and proliferation of VSMCs, which would promote neointimal hyperplasia, and thus, restenosis occurred. In our study, Telmisartan, a specific AT_1R blocker, might inhibit the migration and proliferation of VSMCs, which led to neointimal hyperplasia, by down-regulating the expression of Cx43 in vascular wall. Taking all the results above into consideration, we supposed that Telmisartan might play a key role in the prevention of restenosis after PCI.

Funding The present study was supported by the Tianjin Municipal Health Bureau Science and Technology Foundation (no. 2010KZ61 and Grant no. 2013KR18).

Compliance with ethical standards

Ethical approval All applicable international, national, and/or institutional guidelines for the care and use of animals were followed. All procedures performed in studies involving animals were in accordance with the ethical standards of the institution or practice at which the studies were conducted. This article does not contain any studies with human participants performed by any of the authors.

Conflict of Interest The authors declare no potential conflict of interest.

References

1. Jukema JW, Verscuren JJ, Ahmed TA, Quax PH (2011) Restenosis after PCI. Part 1: pathophysiology and risk factors. Nat Rev Cardiol 9:53–62

2. Alfonso F, Byrne RA, Rivero F, Kastrati A (2014) Current treatment of in-stent restenosis. J Am Coll Cardiol 63:2659–2673
3. Byrne RA, Joner M, Kastrati A (2015) Stent thrombosis and restenosis: what have we learned and where are we going? The Andreas Grüntzig Lecture ESC 2014. Eur Heart J 36:3320–3331
4. Canfield J, Totary-Jain H (2018) 40 years of percutaneous coronary intervention: history and future directions. J Pers Med 8:E33
5. Pourdjabbar A, Hibbert B, Simard T, Ma X, O'Brien E (2011) Pathogenesis of neointima formation following vascular injury. Cardiovasc Hematol Disord Drug Targets 11:30–39
6. Liu ZJ, Shi B, Deng CC, Xu GX, Zhao RZ, Chen CY, Wang ZL, Liu HL (2017) Analysis of optical coherence tomography of early and very late stent restenosis after drug-eluting stent implantation. Natl Med J China 97:1778–1783
7. Chaabane C, Otsuka F, Virmani R, Bochaton-Piallat ML (2013) Biological responses in stented arteries. Cardiovasc Res 99:353–363
8. Marx SO, Totary-Jain H, Marks AR (2011) Vascular smooth muscle cell proliferation in restenosis. Circ Cardiovasc Interv 4:104–111
9. Wu BJ, Li Y, Ong KL, Sun Y, Shrestha S, Hou L, Johns D, Barter PJ, Rye KA (2017) Reduction of in-stent restenosis by cholesteryl ester transfer protein inhibition. Arterioscler Thromb Vasc Biol 37:2333–2341
10. Bennett MR, Sinha S, Owens GK (2016) Vascular smooth muscle cells in atherosclerosis. Circ Res 118:692–702
11. Brisset AC, Isakson BE, Kwak BR (2009) Connexins in vascular physiology and pathology. Antioxid Redox Signal 11:267–282
12. Morel S, Kwak BR (2013) Vascular connexins in restenosis after baloon injury. Methods Mol Biol 1037:381–398
13. Leybaert L, Lampe PD, Dhein S, Kwak BR, Ferdinandy P, Beyer EC, Laird DW, Naus CC, Green CR, Schulz R (2017) Connexins in cardiovascular and neurovascular health and disease: pharmacological implications. Pharmacol Rev 69:396–478
14. Li X, Simard JM (1999) Multiple connexins form gap junction channels in rat basilar artery smooth muscle cells. Circ Res 84:1277–1284
15. Begandt D, Good ME, Keller AS, DeLalio LJ, Rowley C, Isakson BE, Figueroa XF (2017) Pannexin channel and connexin hemichannel expression in vascular function and inflammation. BMC Cell Biol 18:2
16. Okamoto T, Suzuki K (2017) The role of gap junction-mediated endothelial cell-cell interaction in the crosstalk between inflammation and blood coagulation. Int J Mol Sci 18:2254
17. Déglise S, Martin D, Probst H, Saucy F, Hayoz D, Waeber G, Nicod P, Ris HB, Corpataux JM, Haefliger JA (2005) Increased connexin43 expression in human saphenous veins in culture is associated with intimal hyperplasia. J Vasc Surg 41:1043–1052
18. Han XJ, Chen M, Hong T, Zhu LY, He D, Feng JG, Jiang LP (2015) Lentivirus-mediated RNAi knockdown of the gap junction protein, Cx43, attenuates the development of vascular restenosis following balloon injury. Int J Mol Med 35:885–892
19. Han XJ, He D, Xu LJ, Chen M, Wang YQ, Feng JG, Wei MJ, Hong T, Jiang LP (2015) Knockdown of connexin 43 attenuates balloon injury-induced vascular restenosis through the inhibition of the proliferation and migration of vascular smooth muscle cells. Int J Mol Med 36:1361–1368
20. Wang LJ, Liu WD, Zhang L, Ma KT, Zhao L, Shi WY, Zhang WW, Wang YZ, Li L, Si JQ (2016) Enhanced expression of Cx43 and gap junction communication in vascular smooth muscle cells of spontaneously hypertensive rats. Mol Med Rep 14:4083–4090
21. Bruder-Nascimento T, Chinnasamy P, Riascos-Bernal DF, Cau SB, Callera GE, Touyz RM, Tostes RC, Sibinga NE (2014) Angiotensin II induces Fat1expresion/activation and vascular smooth muscle cellmigration via Nox1dependent reactive oxygen species generation. J Mol Cell Cardiol 66:18–26
22. Rinfret S, Baron SJ, Cohen DJ (2015) Percutaneous coronary intervention: finally mature enough. J Am Coll Cardiol 65:2508–2510
23. Faxon DP, Williams DO (2016) Interventional cardiology: current status and future directions in coronary disease and valvular heart disease. Circulation 133:2697–2711
24. Buccheri D, Piraino D, Andolina G, Cortese B (2016) Understanding and managing in-stent restenosis: a review of clinical data, from pathogenesis to treatment. J Thorac Dis 8:E1150–E1162
25. Allahverdian S, Chaabane C, Boukais K, Francis GA, Bochaton-Piallat ML (2018) Smooth muscle cell fate and plasticity in atherosclerosis. Cardiovasc Res 114:540–550
26. Chistiakov DA, Orekhov AN, Bobryshev YV (2015) Vascular smooth muscle cell in atherosclerosis. Acta Physiol 214:33–50
27. Denes L, Entz L, Jancsika V (2012) Restenosis and therapy. Int J Vasc Med 2012:406236
28. Lacolley P, Regnault V, Nicoletti A, Li Z, Michel JB (2012) The vascular smooth muscle cell in arterial pathology: a cell that can take on multiple roles. Cardiovasc Res 95:194–204
29. Nikol S, Huehns TY, Höfling B (1996) Molecular biology and post-angioplasty restenosis. Atherosclerosis 123:17–31
30. Yeh HI, Lupu F, Dupont E, Severs NJ (1997) Upregulation of connexin43 gap junctions between smooth muscle cells after balloon catheter injury in the rat carotid artery. Arterioscler Thromb Vasc Biol 17:3174–3184
31. Zhang XM, Wang XD, Zhou XH, Ma XY, Yao Y, Liu XB (2016) Phenotypic transformation of smooth muscle cells from porcine coronary arteries is associated with connexin 43. Mol Med Rep 14:41–48
32. Nagayama K, Kyotani Y, Zhao J, Ito S, Ozawa K, Bolstad FA, Yoshizumi M (2015) Exendin-4 prevents vascular smooth muscle cell proliferation and migration by angiotensin II via the Inhibition of ERK1/2 and JNK signaling pathways. PLoS ONE 10:e0137960
33. Liu G, Hitomi H, Rahman A, Nakano D, Mori H, Masaki T, Ma H, Iwamoto T, Kobori H, Nishiyama A (2014) High sodium augments angiotensin II-induced vascular smooth muscle cell proliferation through the ERK 1/2-dependent pathway. Hypertens Res 37:13–18
34. Montezano AC, Nguyen Dinh Cat A, Rios FJ, Touyz RM (2014) Angiotensin II and vascular injury. Curr Hypertens Rep 16:431
35. Jia G, Cheng G, Gangahar DM, Agrawal DK (2008) Involvement of connexin 43 in angiotensin II-induced migration and proliferation of saphenous vein smooth muscle cells via the MAPK-AP-1 signaling pathway. J Mol Cell Cardiol 44:882–890
36. Alonso F, Krattinger N, Mazzloai L, Simon A, Waeber G, Meda P, Haefliger JA (2010) An angiotensionII-and NF-Kb-dependent mechanism increases connexin 43 in murine arteries targeted by renin-dependent hypertension. Cardiovasc Res 87:166–176
37. Hou J, Yan P, Guo T, Xing Y, Zheng S, Zhou C, Huang H, Long H, Zhong T, Wu Q, Wang J, Wang T (2015) Cardiac stem cells transplantation enhances the expression of connexin 43 via the ANG II/AT1R/TGF-beta1 signaling pathway in a rat model of myocardial infarction. Exp Mol Pathol 99:693–701
38. Liu C, Fan Y, Zhou L, Zhu HY, Song YC, Hu L, Wang Y, Li QP (2015) Pretreatment of mesenchymal stem cells with angiotensin II enhances paracrine effects, angiogenesis, gap junction formation and therapeutic efficacy for myocardial infarction. Int J Cardiol 188:22–32
39. Mueck AO, Seeqer H, Lippert TH (1999) Valsartan inhibits angiotensin II-stimulated proliferation of smooth muscle cells from human coronary artery. Int J Clin Pharmacol Ther 37:365–366
40. Peters S, Götting B, Trömmel M, Rust H, Brattström A (2001) Valsartan for prevention of restenosis after stenting of type B2/C lesions: the VAL-PREST trial. J Invasive Cardiol 13:93–97
41. Valente AJ, Yoshida T, Murthy SN, Sakamuri SS, Katsuyama M, Clark RA, Delafontaine P, Chandrasekar B (2012) Angiotensin

II enhances AT1-Nox1 binding and stimulates arterial smooth muscle cell migration and proliferation through AT1, Nox1, and interleukin-18. Am J Physiol Heart Circ Physiol 303:H282–H296
42. Ichikawa N, Toma N, Kawakita F, Matsushima S, Imanaka-Yoshida K, Yoshida T, Taki W, Suzuki HI (2015) Angiotensin II type 1 receptor blockers suppress neointimal hyperplasia after stent implantation in carotid arteries of hypercholesterolemic rabbits. Neurol Res 37:147–152
43. Cho JY, Hong SJ, Lim DS (2017) Effects of angiotensin receptor blockers on neointimal characteristics in angina patients requiring stent implantation: optical coherence tomography analysis. BMC Cardiovasc Disord 17:278
44. Kun X, Yong L, Bo J, Hai-Ming S (2011) Neointimal hyperplasia inhibition effect of angiotensin II type 1 receptor blockers in patients after coronary stent implantation: a meta-analysis. Am J Cardiovasc Drugs 11:209–213